Microporous and Mesoporous Materials 223 (2016) 261–267

Contents lists available at ScienceDirect

Microporous and Mesoporous Materials

journal homepage: www.elsevier.com/locate/micromeso

In-situ synthesis and characterization of V-MCM-41 for oxidative dehydrogenation of n-butane

Xiaosheng Wang, Guanglin Zhou, Zhiwei Chen, Weili Jiang, Hongjun Zhou*

Institute of New Energy, State Key Laboratory of Heavy Oil Processing, China University of Petroleum, Beijing, China

ARTICLE INFO

Article history:
Received 27 March 2014
Received in revised form
19 June 2015
Accepted 23 June 2015
Available online 2 July 2015

Keywords:
In-situ synthesis
V-MCM-41
n-Butane
Oxidative dehydrogenation

ABSTRACT

A series of MCM-41 catalysts with different vanadium content were prepared via prehydrolysis hydrothermal method with ammonia metavanadate as precursors. The prepared samples were characterized by Powder X-ray diffraction (XRD), N_2 adsorption–desorption, X-ray photoelectron spectra (XPS), H_2 temperature-programmed reduction (TPR), scanning electron microscopy (SEM) and transmission electron microscopy (TEM). Results showed that V-MCM-41 could still maintain hexagonal mesoporous structure and large specific surface area when the vanadium content was low, whereas the mesoporous structure collapsed in the high V-containing samples. Two vanadium species ($V^{5+}/VSiO_x$ and V^{5+}/V_2O_5) were identified in the catalysts and the highly dispersed vanadium species decreased with the increasing vanadium content. The activity of the catalysts were tested for the oxidative dehydrogenation (ODH) of n-butane with O_2 as oxidant, the results showed that $V^{5+}/VSiO_x$ was more active than V^{5+}/V_2O_5.

1. Introduction

In the last decade, the oxidative dehydrogenation (ODH) of light alkanes has aroused great interests all over the world. The ODH reaction provides a promising alternation to thermal cracking in producing corresponding alkenes [1,2]. Compared with the traditional oxygen-free dehydrogenation process, the ODH reaction is thermodynamically favourable and not limited by reaction equilibrium. Besides, the oxidant in the feedstock and water produced by the reaction might prevent or slow down the carbon deposition and hence can prolong the life span of the catalysts [3]. Up to now, considerable amount of work had been carried out to find a catalyst with high conversion of light alkanes and selectivity to alkenes [1,4–6]. Al_2O_3, MgO and SiO_2 supported V-based catalysts have been pervasively used to the dehydrogenation of ethane, propane, and butanes. Among these catalysts, the vanadium-loaded mesoporous silicate (especially M41s) showed excellent performances for the ODH reaction. MCM-41, which was the first ordered mesoporous silicate and the most famous member of the M41s family, was first synthesized by Kresge [7] in 1990s and then used as support pervasively. Due to its large specific surface area and highly ordered hexagonal structure with controllable pore diameter from 2 to 10 nm [8–10], MCM-41 is far better in mass transfer compared with traditional zeolites and other metal oxides.

Various vanadium modified MCM-41 catalysts were reported in the literature for the synthesis of olefins. It had been recognized that the dispersion and structure of the vanadium species was an important factor responsible for the catalytic activity of ODH reaction [11,12]. Bulánek reported that vanadium species formed in the catalysts could be separated into four types, namely isolated monomeric units (tetrahedral coordination), one-dimensional oligomeric units (distorted tetrahedral coordination), two-dimensional polymeric units (octahedral coordination) and three-dimensional V_2O_5 crystallites [11]. The former three types were more active and selective for the ODH reaction and stood for highly dispersed vanadium species. To take advantage of the textural characteristics of MCM-41, methods such as impregnation [13], template-ion exchange [14] and direct hydrothermal synthesis [9] had been adopted to introduce vanadium into the molecular sieves. By adding vanadium precursors directly into the parent gel, direct hydrothermal synthesis was believed to be more effective in enhancing the dispersion of vanadium species.

In this paper, method of modified hydrothermal synthesis was used to prepare vanadium-containing MCM-41. During the synthesis process, the silica source was added to the vanadium-oxalic acid solution and pre-hydrolyzed to form a homogeneous gel solution. The materials thus obtained were characterized by means of XRD, N_2 adsorption–desorption, H_2-TPR, XPS, SEM and TEM.

---

* Corresponding author.
E-mail address: zhouhongjun63@126.com (H. Zhou).

http://dx.doi.org/10.1016/j.micromeso.2015.06.029
1387-1811/

Moreover, the catalytic performance of the catalysts was also investigated for the ODH of n-butane.

2. Experimental

2.1. Catalyst synthesis

V-MCM-41 catalysts were prepared by direct hydrothermal method according to literature [15] with some modifications. Typically, 12.5 g of cetyl trimethyl ammonium bromide (CTAB, A.R., Sinopharm) and 75 g of ammonia solution (25%, A.R., Beijing Chemical Works) were added to 600 g of deionized water and stirred thoroughly until a clear solution was obtained, denoted as solution A. Then a solution containing certain amount of ammonium metavanadate (NH_4VO_3, A.R., Sinopharm) and oxalic acid ($H_2C_2O_4 \cdot 2H_2O$, A.R, Sinopharm) with the molar ratio of 1/2 was heated to 90 °C for 30 min, followed by adding 60 g of tetraethyl orthosilicate (TEOS, A.R., Sinopharm) and pre-hydrolyzed till a homogeneous solution was obtained, denoted as solution B. Solution B was added into solution A dropwise under vigorous stirring and the resultant homogeneous reaction mixture was stirred for another 8 h before transferring into stainless-steel autoclaves and crystallized at 120 °C for 72 h under static conditions. The solid was filtered out and washed with copious amounts of water. The materials were then dried at 120 °C for 10 h and calcined at 550 °C for 6 h with a heating ramp of 1 °C/min. The samples were denoted as xV-MCM-41, where x represents the V weight percentage in the calcined catalysts.

2.2. Catalysts characterization

Powder X-ray diffraction (XRD) patterns of the catalysts were obtained on a D8 Advance (Bruker) X-ray diffractometer provided with Ni filtered Cu-Kα (λ = 0.15416 nm) radiation at 40 kV and 30 mA. The scanning speed was 5 °C/min in the range of 1.3–50°.

N_2 adsorption–desorption isotherms of the catalysts were performed on an ASAP 2020 (Micromerities) instrument to examine the pore properties. The samples were pretreated at 90 °C for 1 h and then degassed at 5.7×10^2 Pa, 350 °C for 5 h. The specific surface area was determined by the Brunauer–Emmett–Teller (BET) method and the pore volume and pore size distribution were derived from the adsorption isotherms using the Barret–Joyner–Halanda (BJH) method.

The real vanadium content was determined by inductively coupled plasma-optical emission spectrometry (ICP-OES) after macro-assisted dissolution of the samples in HF/HNO_3 mixed solution.

X-ray photoelectron spectra (XPS) were recorded with a K-Alpha (Thermo Fisher) instrument equipped with a multichannel hemispherical electron analyzer, using Al Kα as the exciting radiation at constant pass energy of 149.814 eV. The pressure in the chamber was maintained bellowed 5×10^{-7} Pa and the charge compensation was done with the adventitious C1s peak at 284.6 eV.

H_2 temperature-programmed reduction (H_2-TPR) was performed on an Autochem 2920 (Micromerities) in the range of 100–800 °C. Samples (100 mg) were first treated in dry air at 500 °C for 1 h then cooled down to ambient temperature in N_2 atmosphere before being reduced in a flow of H_2/Ar (10%H_2 and a total flow of 50 ml min^{-1}). The samples were heated up to 800 °C at a rate of 10 °C•min^{-1} and the effluent was monitored by a TCD detector.

SEM and TEM images were collected with a Quanta Chrome 200-F and a JEOL JEM-2100 LaB_6 microscope respectively. The samples were coated with gold before the SEM examination.

2.3. Catalysts test

The n-butane oxidative dehydrogenation (ODH) reaction was carried out in a fixed-bed reactor made of stainless steel tube (length: 60 cm, inner diameter: 14 mm) at atmospheric pressure. The feed composition was n-butane/O_2/N_2 = 2/1/4 and the reaction temperature (550 °C), overall hourly space velocity (500 ml g_{cat}^{-1} h^{-1}) and n-butane to oxygen ratio were kept constant. In a typical experiment, 5 g catalyst was installed in the isothermal region of the reactor and pretreated at 450 °C for 2 h in an air stream prior to be heated up to 550 °C. The outlet gases were analyzed on-line by a gas chromatograph equipped with FID (Agilent GS-Alumina capillary column, 30 m × 0.53 mm) for hydrocarbons and TCD (TDX-01 packed column, 2 m × 0.3 mm) for permanent gases. The feed conversion and selectivity to products were calculated on the basis of carbon balance (coke deposited omitted).

3. Results and discussion

3.1. Characterization of catalysts

XRD patterns of V-MCM-41 samples were shown in Figs. 1 and 2. Small-angle XRD patterns of purely silicious MCM-41 (Fig. 1a) showed three well-resolved diffraction peaks at 2θ = 2.3°, 3.7° and 4.4°, corresponding to the (100), (110) and (200) crystal surface of highly ordered hexagonal mesoporous structure [9]. The peak intensity of the Vanadium-containing samples were not so strong as the purely silicious one and became even lower with further rise in vanadium loading. This indicated that the long-range regularity of hexagonal arrays of mesopores was declined by the introduction of vanadium ions [16]. Furthermore, the disappearance of diffraction peaks indexed to (100), (110) and (200) in 12V-MCM-41 suggested that the hexagonal structures were largely damaged [5]. This was maybe caused by the metal ions introduction into the material which could hinder the structure directing action of template in the solution [12]. Another trend that obviously can be summarized from Fig. 1 was the diffraction peaks of (100) in the 2θ range of 2.0°–2.3° shifted slightly to lower angle. The d_{100} spacing (shown in Table 1) was also widened as the V content increased [9]. Large angle XRD patterns were shown in Fig. 2. Only a broad peak due to amorphous feature of MCM-41 framework was observed. There

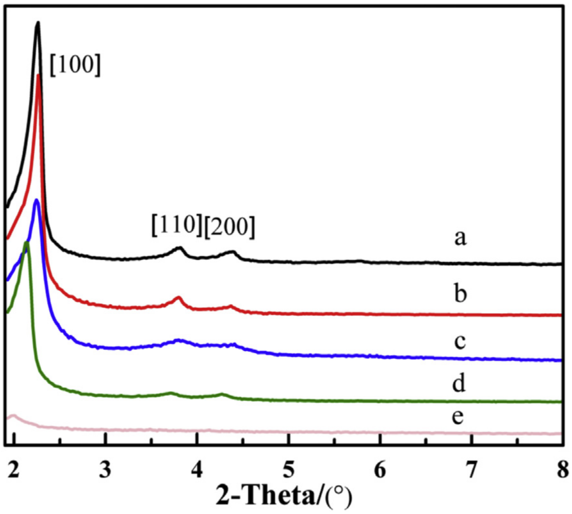

Fig. 1. Small-angle XRD patterns of V-MCM-41 samples. a. MCM-41; b. 3V-MCM-41; c. 6V-MCM-41; d. 9V-MCM-41; e. 12V-MCM-41.